JOURNAL OF MAGNETIC RESONANCE **134,** 355–359 (1998)
ARTICLE NO. MN981528

Pulsed Field Gradient Selection in Two-Dimensional Magic Angle Spinning NMR Spectroscopy of Dipolar Solids

Tilo Fritzhanns,* Siegfried Hafner,* Dan E. Demco,*,[1] Hans W. Spiess,* and Frank H. Laukien†

*Max-Planck-Institut für Polymerforschung, Postfach 3148, D-55021, Mainz, Germany; and
†Bruker Instruments, Inc., Manning Park, Billerica, Massachusetts 01821

Received March 24, 1998; revised May 20, 1998

The utility of gradient selection in MAS spectroscopy of dipolar solids is explored in two examples. In the first, rotor-synchronized gradients of appropriate strength and duration are applied to select ^{1}H double-quantum coherences. The resulting DQ MAS spectrum of adamantane is compared with that acquired by the corresponding phase-cycling technique. As a second example, a ^{1}H 2D exchange MAS experiment is performed on an elastomer sample. In this experiment, a gradient is applied to remove undesired coherences that would otherwise distort the spectrum for short mixing times. The diagonal-peak intensities in the resulting spectrum show a linear decrease with increasing mixing time indicating cross-relaxation by slow chain motions as the relevant process. Both types of experiments demonstrate the potential of gradient-selection techniques for MAS spectroscopy of dipolar solids.

High-resolution solid-state NMR spectroscopy is an important tool for the study of structure, molecular dynamics and molecular orientation in dipolar and quadrupolar solids (*1*). Although most applications to date have focused on ^{13}C MAS spectroscopy, there has also been progress concerning high-resolution spectroscopy of protons in rigid solids. Fast magic angle sample spinning (MAS) alone or in combination with coherent-averaging multiple-pulse sequences can be used to increase resolution and sensitivity (*2*). Moreover, using suitable dipolar recoupling techniques, dipolar couplings can be reintroduced again during parts of a fast MAS experiment which allows couplings and distances to be measured site selectively (*3*). A prominent example of such experiments is given by multiple-quantum MAS spectroscopy where applications to homonuclear (*2, 4–8*) and heteronuclear (*9*) systems have been already shown. Both aspects, the decoupling and the possibility for recoupling of parts of the interaction, make fast MAS spectroscopy a promising tool for the investigation of materials.

While the selection of coherences in these experiments usually is performed by phase cycling (*10*), coherence-pathway selection can also be achieved by use of pulsed field gradients (PFGs) as is well-established in high-resolution solution NMR spectroscopy (for recent reviews see for instance Refs. (*11, 12*)). Although pulsed field gradients have been used in solid-state MAS imaging (*13, 14*), it was only recently that field gradients were combined with magic-angle spinning for spectroscopic purposes. As an early example, a heteronuclear correlation (HETCOR) gradient-MAS experiment was performed on swollen resins (*15*) to show that PFGs can reduce t_1 noise due to probe geometry and sample spinning which would otherwise lead to pronounced spectral artifacts. Also in MQ-MAS spectroscopy of half-integer quadrupole nuclei (*16–19*) PFGs have been used already (*20*).

There are some advantages of PFG techniques compared with phase cycling procedures. For instance, coherence selection by PFGs is not based on differences of signals as are the methods using phase cycling. Thus, the full dynamic range of the analog–digital converter can be exploited for the desired signal contributions. Phase cycling procedures in sophisticated pulse techniques tend to be complex, that is, it is often necessary to superimpose a large number of acquisitions until undesired signal contributions finally are eliminated. A pulse sequence utilizing gradients could therefore highly simplify the experiment and save measurement time when signal accumulation is not required anyway for S/N reasons. Further benefits of gradients in NMR spectroscopy are the reduction of t_1 noise (see above) and the elimination of signal contributions from mobile components. The most prominent example for the latter case is the suppression of water signals in solution-state NMR (*21*).

The aim of this work is to explore the use of field gradients for ^{1}H MAS spectroscopy of dipolar solids. Two types of gradient MAS experiments will be investigated. The first is a coherence-transfer-echo (*22, 23*) multiple-quantum (MQ) MAS experiment where the gradient is used for selection of the coherence order while the second is a NOESY-type experiment (*10*) where the gradient filters out undesired transverse coherences during the mixing time.

The experiments were performed on a Bruker DSX 300 NMR spectrometer. A newly designed Bruker gradient MAS probe was used. It has the same RF capability as the 4-mm

[1] Present address: Lehrstuhl für Makromolekulare Chemie, RWTH-Aachen D-52074, Aachen, Germany.

1090-7807/98 $25.00

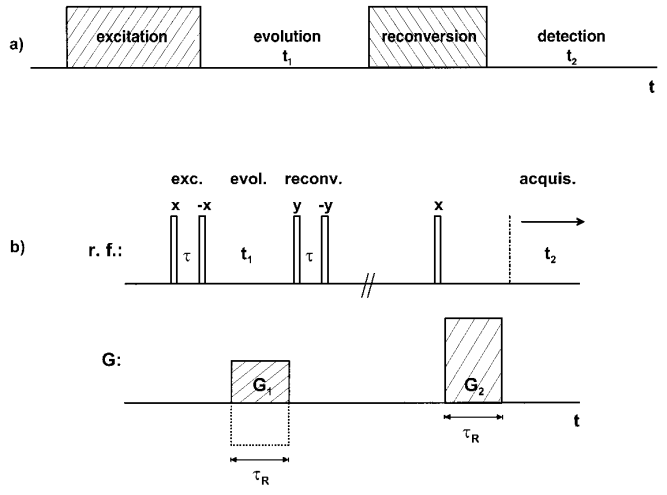

FIG. 1. (a) General scheme of multiple–quantum NMR spectroscopy. (b) Five-pulse sequence used for excitation and reconversion of double-quantum coherences. The applied gradient pulses for the selection of DQ coherences are also shown. In order to obtain absorptive spectra, two experiments with different gradient sign are coadded (the negative gradient is indicated by dotted lines).

CP-MAS probe and uses the gradient technology of the high-resolution MAS probes as described elsewhere (*15*). A field gradient of up to 45 G/cm can be applied in the direction of the rotor axis. This particular direction has the advantage that off-resonance effects caused by the gradient are not modulated by sample rotation. The gradient switching times were determined to be less than 10 μs (at 10% maximum intensity) so that the gradient pulse could be applied within one rotor period for rotor frequencies of up to 15 kHz. Adamantane was used as a representative solid for the MQMAS experiments, while the exchange experiments were performed on a crosslinked styrene-butadiene rubber (SBR). Spinning frequencies of 10 kHz and 8 kHz were used, respectively; this is sufficient for considerable line-narrowing in both cases.

A MQMAS experiment with gradient selection can be performed using the general scheme presented in Fig. 1a. For excitation and reconversion, suitable pulse sequences must be chosen depending on the dipolar-coupling strength found in the investigated material and on the rotor frequency. In this study, a broadband five-pulse sequence (cf. Fig. 1b) was used. For selecting the desired coherence order, gradient pulses are used instead of the usual phase-cycling technique. The sequence of Fig. 1b thus exploits the different sensitivities of the various coherence orders to resonance offsets. More specifically, it takes advantage of the fact that p-quantum coherences dephase p times faster in the presence of a field gradient with strength G than single-quantum coherences do (*11, 12*). After all coherences have been dephased, the desired coherence can be refocused by applying a second gradient pulse with p times the gradient strength G at a later time as shown in Fig. 1b. As an alternative, also a gradient pulse with strength G and p times the duration of the original gradient-pulse length can be applied. In our experiments, however, we used the first procedure which allows rotor synchronization of the gradient pulses with both pulses as short as one rotor period τ_R. Rotor synchronization is not essential when the gradient is applied in the magic-angle direction as long as the crossterms between the dipolar interaction and the gradient are negligible. However, since rotor synchronization does not complicate the experiment, it will nevertheless be used to avoid any influence of such effects.

In order to show the selection of MQ coherences by the field gradients, we consider DQ coherences of a spin-1/2 pair under on-resonance conditions. The treatment is similar to that performed for phase-cycled DQ sequences in Ref. (*6*). For the five-pulse sequence presented in Fig. 1a, the spatially encoded spin-system response for the t_1 period is given by

$$\begin{aligned} S(t_1;\, t_2 = 0;\, z_m) &= \Bigg\{ -\left\langle \cos\left[\sqrt{\frac{3}{2}}\, d(\tau + t_1 + \tau;\, t_1 + \tau) \right] \right. \\ &\quad \times \cos\left[\sqrt{\frac{3}{2}}\, d(\tau;\, 0) \right] + \cos(2k_z \cdot z_m) \\ &\quad \times \left\langle \sin\left[\sqrt{\frac{3}{2}}\, d(\tau + t_1 + \tau;\, t_1 + \tau) \right] \right. \\ &\quad \left. \left. \times \sin\left[\sqrt{\frac{3}{2}}\, d(\tau;\, 0) \right] \right\rangle \right\} \cos(2k_z \cdot z_m), \end{aligned} \qquad [1]$$

where the symbol $\langle\ \rangle$ represents the powder average, $k_z = \gamma G_z \tau_R$ is the wave vector corresponding to a gradient G_z which is applied along the direction of the magic angle, and z_m is the displacement along this direction. The rotor-modulated space part of the dipolar coupling integrated for the time interval $(t''; t')$ is given by

$$\begin{aligned} d(t''; t') = \sum_{m=-2}^{2} (-\sqrt{6})\, D^{ij} d^{(2)}_{-m,0}(\beta_M)\, D^{(2)}_{0,-m}(\alpha^{ij}, \beta^{ij}, \gamma^{ij}) \\ \int_{t'}^{t''} \exp(im\omega_R t)\, dt, \end{aligned} \qquad [2]$$

where $D^{ij} = \mu_0 \gamma^2 \hbar / 4\pi r_{ij}^3$ is the dipolar coupling constant, ω_R is the rotor frequency, β_M is the magic angle, and α^{ij}, β^{ij}, γ^{ij} are the Euler angles relating the principal axes of the dipolar coupling tensor to the reference frame of the rotor. The conventions for the Wigner rotation matrices $D^{(2)}_{m,m'}(\alpha, \beta, \gamma) = \exp(-im\alpha) d^{(2)}_{m,m'}(\beta) \exp(-im'\gamma)$ are those defined in Ref. (*1*), where also the reduced rotation matrix elements $d^{(2)}_{m,m'}(\beta)$ are explicitly given.

The total NMR signal integrated over the sample (denoted below by $\bar{S}$) is given by

$$\bar{S}_{DQ}(t_1;\, t_2 = 0) = \frac{1}{2}\left\langle \sin\left[\sqrt{\frac{3}{2}}\, d(\tau + t_1 + \tau;\, t_1 + \tau) \right] \times \sin\left[\sqrt{\frac{3}{2}}\, d(\tau;\, 0) \right] \right\rangle . \quad [3]$$

The gradient thus filters out the z-magnetization (first term in Eq. [1]) as well as half of the intensity of the double-quantum coherences (this is strictly valid only for a symmetric sample placed in the middle of the gradient coil). The coherence-transfer echo is generated at time τ_R after the read pulse and the filtering efficiency increases with increasing gradient strength.

As a consequence of considering on-resonance conditions, we obtain a pure absorptive signal. Since the gradient is in the argument of the cosine function in Eq. [1], it is obvious that the relative sign of the field gradients is irrelevant, in principle. The spectrum thus can be acquired in a single step. In the real experiment, however, dispersive contributions from chemical shifts and frequency offsets lead to phase distortions which must be compensated by coadding a second acquisition with a negative dephasing gradient (*24*) (see dotted lines in Fig. 1).

In order to demonstrate the use of gradient selection in MQMAS spectroscopy, the experiment of Fig. 1b has been performed by setting the relative gradient strengths $G_2/G_1 = 2$ for selecting double-quantum (DQ) coherences. For comparison, a DQ spectrum with selection by phase cycling was acquired under equivalent experimental conditions. The time t_1 was incremented in 512 steps in both cases and 32 acquisitions were coadded with a repetition time of 3 s. The time τ was chosen to be $\tau_R/2$ to avoid phase distortions. Figure 2 shows the DQ sideband-pattern spectra (*5, 6*) that result after Fourier transformation and phase correction (no further processing of the data was made). In case of selection by phase-cycling (Fig. 2a), phase distortions appear that originate from the finite pulse length which was set to be 3.5 μs for a 90° pulse. These phase problems are obviously removed in the gradient-selected DQ spectrum (Fig. 2b) where, however, small signal contributions are present on the left side that are shifted with respect to the normal DQ sideband pattern. These signal contributions are aliased into the spectral range of the DQ spectrum and originate from the leakage of undesired coherences through the DQ filter because of insufficient gradient strength. Nevertheless, apart from these deviations, both patterns correspond well to each other which once more ensures that DQ sideband patterns (*5, 6*) are genuine and no artifact of the selection technique. They also correspond to the patterns that are expected for spin pairs perturbed by dipolar couplings to remote spins (*6*).

The second gradient-MAS experiment, a NOESY-type experiment, exploits a spoil gradient for removing transverse components during the mixing time. Figure 3 shows the basic pulse program, a three-pulse exchange sequence. It corresponds to the exchange experiment performed in Ref. (*25*) with the only exception that it is now applied under high-resolution

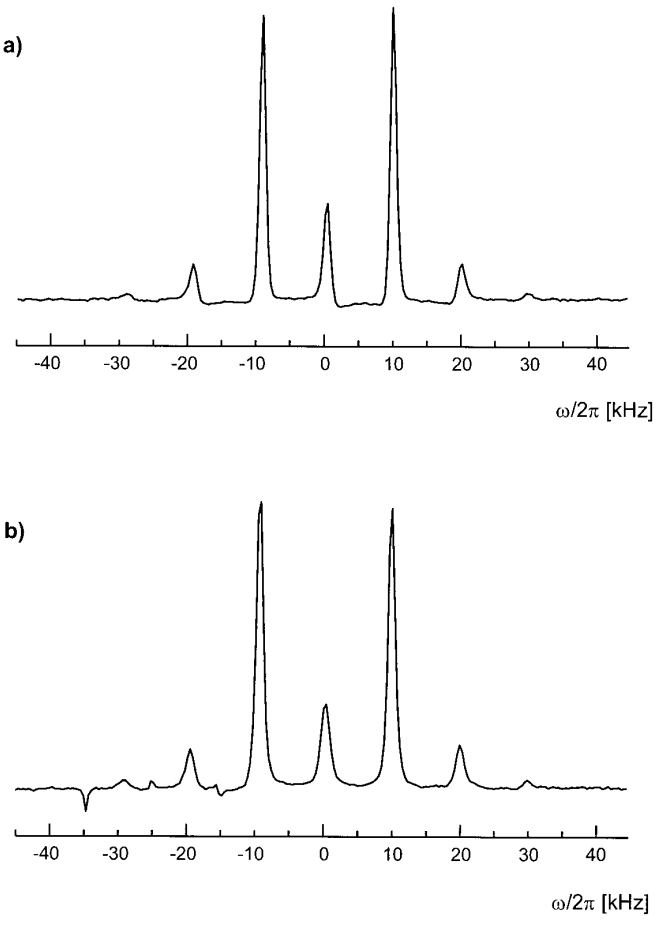

FIG. 2. Proton DQ spinning-sideband patterns of an adamantane sample acquired at 10 kHz (normalized to the same height). (a) Spectrum with DQ selection by phase cycling. (b) Spectrum with gradient selection of the double-quantum coherence.

MAS conditions. In order to avoid unnecessary complications due to sample rotation, the mixing time t_m is chosen to be a multiple of the rotor period. Since the free-induction decay of elastomers under MAS is relatively long, it is important that the transverse components of the magnetization are filtered out when the mixing times are short. For this reason the gradient is applied during the mixing time.

As was already outlined in Ref. (*25*), there are two processes to be considered which could lead to the generation of cross-peaks between the different lines in the exchange spectrum of an elastomer sample. The first is a coherent exchange process mediated by a constant residual dipolar coupling while the other corresponds to cross-relaxation due to the fluctuating part of the dipolar interaction. As was shown in Ref. (*25*) the coherent-exchange process can be selectively investigated for static samples using the fact that it dominates the initial part of the decay. Under fast MAS conditions, however, the coherent exchange is largely refocused for full rotor periods and therefore does not influence the decay to first order. In this case, a pure NOESY type spectrum should result even for short mix-

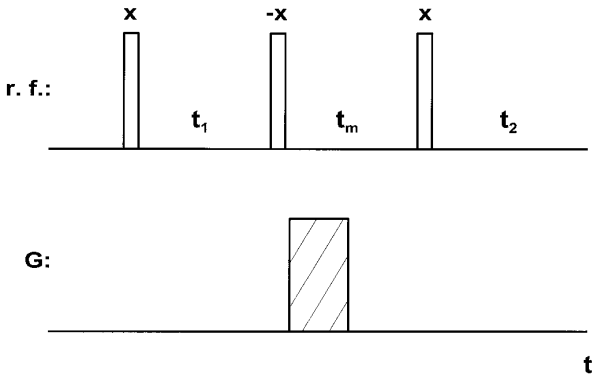

FIG. 3. Pulse scheme for 2D-exchange MAS spectroscopy used in the experiments. A spoil gradient is applied during the mixing time to select for longitudinal magnetization.

ing times so that now the cross-relaxation by the fluctuating part of the dipolar interaction can be studied.

Figure 4 shows the 2D spectra of a SBR sample acquired with a mixing time of 4 ms. The relevant lines in the 8 kHz MAS spectra are well resolved. They can be assigned as is indicated in Fig. 4. Already at the short mixing time of 4 ms pronounced crosspeaks are visible. The first 2D spectrum, Fig. 4a, has been acquired without application of the gradient but with a phase cycle for correcting quadrature balance imperfections (CYCLOPS) and T_1 relaxation. A repetition time of 1 s was chosen which is about twice T_1. The experiment was performed using time-proportional phase-incrementation and 256 t_1 increments were found to be sufficient to resolve the spectrum. While the desired part of the signal stems from longitudinal magnetization during the mixing period, obviously also transverse components survive the 4 ms mixing time and lead to pronounced phase distortions, for instance in the region around 5 ppm. In order to avoid these phase distortions, a short gradient pulse of length τ_R is applied in the mixing period. Figure 4b shows the corresponding spectrum which was acquired with the same number of acquisitions and is practically free from phase distortions. A phase cycling scheme for eliminating these effects would be four times longer.

Since the time required for the 2D exchange spectra with gradient selection is relatively short for the investigated samples (around one hour), a series of such spectra with increasing mixing time could be acquired overnight. From such a series of 2D spectra, the decay of the diagonal peaks or the build-up of the crosspeaks can be evaluated. As a representative example for the three main diagonal peaks, Fig. 5 shows the decay curve for the CH peak for short mixing times. It is found to be approximately linear in contrast to the short-time behavior of the static exchange experiment which is quadratic. While in the static case, the initial magnetization-exchange process is dominated by coherent exchange, cross-relaxation effects obviously dominate under MAS conditions and lead to a linear dependence for short mixing times (Refs. (*25, 26*)) as is indeed observed in Fig. 5. Moreover, the positive crosspeaks are a clear indication of slow chain motions.

In conclusion, the applicability of gradient-selection methods to solid-state NMR MAS spectroscopy has been shown for two representative examples. The advantages of gradient selection were found to apply equally well to the case of solid-state MAS spectroscopy as to high-resolution spectroscopy of liquids. In particular, complicated phase-cycling techniques, t_1-noise, and dynamic-range problems of the digitizer can be avoided.

In the case of modestly rigid solids, the use of gradients for the selection of MQ coherences provides an attractive alternative to phase-cycling procedures. Also, for particularly com-

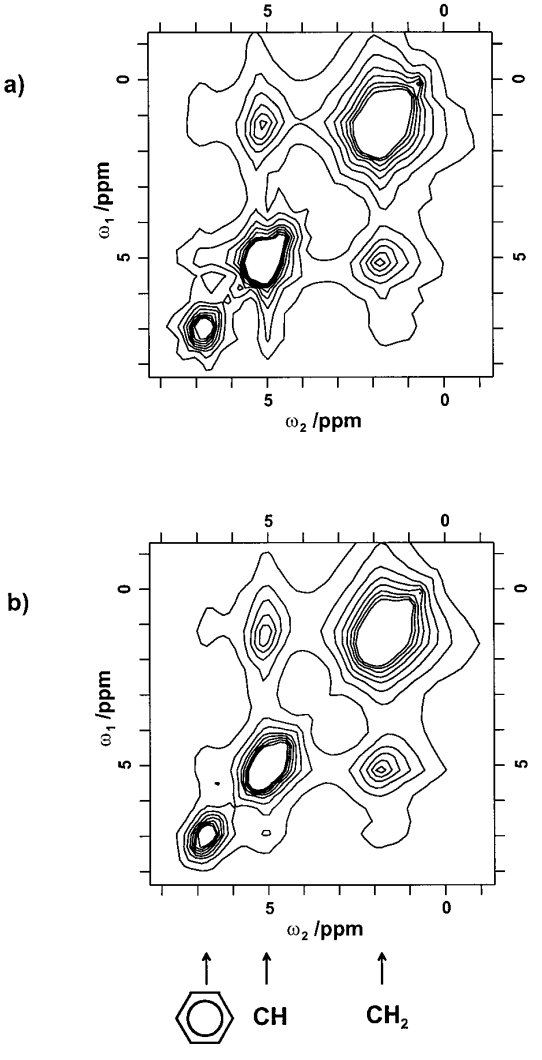

FIG. 4. ^{1}H 2D exchange spectra of a SBR sample acquired under MAS conditions for a mixing time of 4 ms. (a) Spectrum without gradient. Phase distortions prevent quantitative evaluation of the exchange peaks. (b) Spectrum with spoil gradient applied during the mixing time of the experiment. In both spectra the contour levels are shown for the range of 4–26% of the maximum peak intensity to allow a convenient comparison of the crosspeak intensities.

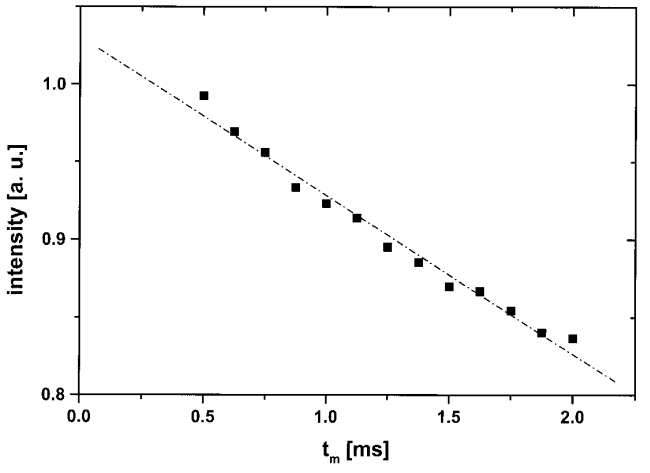

FIG. 5. Initial decay of the CH diagonal peak intensity in a 2D exchange spectrum of a SBR sample as a function of the mixing time. The decay is found to be linear within the error limits indicating that cross-relaxation by slow chain motions is the relevant process.

plicated pulse sequences both techniques can be combined to avoid long phase-cycling schemes. In the 2D exchange spectroscopy experiment, a spoil gradient is sufficient to clean the detected signal from phase distortions by removing the transverse components and multiple-quantum coherences during the mixing time. Together with MAS, this allows the separation of the NOE effect from the coherent magnetization exchange even for short mixing times, where a linear approximation can be used for evaluating cross-relaxation rates.

The experiments discussed above demonstrate that gradient-selection techniques have considerable potential for simplifying solid-state NMR techniques under MAS conditions. The main limitation so far is the duration of the gradient pulses which is determined by the achievable gradient strength and the gradient switching times. For the latter reason, RF-field gradients (*11*) might be an alternative to static magnetic-field gradients.

ACKNOWLEDGMENTS

Financial support by the Deutsche Forschungsgemeinschaft is gratefully acknowledged. D.E.D. thanks the Alexander von Humbold Stiftung for a research award. The authors thank S. De Paul, S. Brown, I. Schnell, D.G. Burum, and M. Ziliox for helpful discussions.

REFERENCES

1. K. Schmidt-Rohr and H.W. Spiess, "Multidimensional Solid State NMR and Polymers," Academic Press, New York (1994).
2. S. Hafner, and H. W. Spiess, *Concepts Magn. Reson.* **10,** 99–128 (1998).
3. A. E. Bennett, R. G. Griffin, and S. Vega, *NMR Basis Principles Prog.* **33,** 3 (1994).
4. Y. K. Lee, N. D. Kurur, M. Helmle, O. G. Johannessen, N. C. Nielsen, and M. H. Levitt, *Chem. Phys. Lett.* **242,** 304 (1995).
5. H. Geen, J. Titman, J. Gottwald, and H. W. Spiess, *J. Magn. Reson. A* **114,** 264 (1995).
6. J. Gottwald, D. E. Demco, R. Graf, and H. W. Spiess, *Chem. Phys. Lett.* **243,** 314 (1995).
7. S. Ding and C. A. McDowell, *J. Magn. Reson. A* **120,** 261 (1996).
8. R. Graf, D. E. Demco, J. Gottwald, S. Hafner, and H. W. Spiess, *J. Chem. Phys.* **106,** 885 (1997).
9. W. Sommer, J. Gottwald, D. E. Demco, and H. W. Spiess, *J. Magn. Reson. A* **112,** 131 (1995).
10. R. R. Ernst, G. Bodenhausen, and A. Wokaun, "Principles of Nuclear Magnetic Resonance in One and Two Dimensions," Oxford University Press, Oxford (1987).
11. D. Canet, *Prog. NMR Spectrosc.* **30,** 101 (1997).
12. S. Berger, *Prog. NMR Spectrosc.* **30,** 137 (1997).
13. D. G. Cory and W. S. Veeman, *J. Phys. E Sci. Instrum.* **22,** 180 (1989).
14. U. Scheler, G. Schauss, B. Blümich, and H. W. Spiess, *Solid State NMR* **6,** 375 (1996).
15. W. E. Maas, F. H. Laukien, and D. G. Cory, *J. Am. Chem. Soc.* **118,** 13,085 (1996).
16. L. Frydman and J. S. Harwood, *J. Am. Chem. Phys.* **67,** 1752 (1995).
17. C. Fernandez and J. Amoureux, *Chem. Phys. Lett.* **242,** 449 (1995).
18. D. Massiot, B. Touzo, D. Trumeau, J. P. Coutures, J. Virlet, P. Florian, and P. J. Grandinetti, *Solid State NMR* **6,** 73 (1996).
19. S. P. Brown and S. Wimperis, *J. Magn. Reson.* **128,** 42 (1997).
20. C. A. Fyfe, J. Skibsted, H. Grondey and H. Meyer zu Altenschilde, *Chem. Phys. Lett.* **281,** 44 (1997).
21. P. C. M. van Zijl and C. T. W. Moonen, *J. Magn. Reson.* **87,** 18 (1990).
22. M. Munowitz and Pines, *Adv. Chem. Phys.* **66,** 1 (1987).
23. D. P. Weitekamp, *Adv. Magn. Reson.* **11,** 111 (1993).
24. R. E. Hurd, B. K. John, and H. D. Plant, *J. Magn. Reson.* **93,** 666 (1991).
25. D. E. Demco, S. Hafner, C. Fülber, R. Graf, and H. W. Spiess, *J. Chem. Phys.* **105,** 11,285 (1996).
26. D. Canet, "Nuclear Magnetic Resonance: Concepts and Methods," Wiley, Chichester (1996).